Evolution of $L1_2$ ordered domains in fcc Cu_3Au alloy

2007 J. Phys.: Condens. Matter 19 086201

(http://iopscience.iop.org/0953-8984/19/8/086201)

INSTITUTE OF PHYSICS PUBLISHING JOURNAL OF PHYSICS: CONDENSED MATTER

J. Phys.: Condens. Matter **19** (2007) 086201 (9pp) doi:10.1088/0953-8984/19/8/086201

Evolution of $L1_2$ ordered domains in fcc Cu_3Au alloy

Mahdi Sanati[1,2] **and Alex Zunger**[2]

[1] Physics Department, Texas Tech University, Lubbock, TX 79409, USA
[2] National Renewable Energy Laboratory, Golden, CO 80401, USA

Received 26 September 2006, in final form 12 December 2006
Published 6 February 2007
Online at stacks.iop.org/JPhysCM/19/086201

Abstract

When a disordered $Cu_{0.75}Au_{0.25}$ alloy is cooled down below T_c (=663 K), it orders into the $L1_2$ phase (Cu_3Au), exhibiting initially a microstructure of domain walls. Whereas at long time (t) the average size of the domains develops as a power law $\propto t^{1/2}$, at short times a distinct incubation period is observed experimentally. We show that a first-principles description of a configurational Hamiltonian via the 'mixed-space cluster expansion' that includes both 'chemical' and 'strain' effects produces such an incubation period in Monte Carlo simulations, whereas the classical short-ranged ('chemical' only) Ising description does not. We find that the origin of this delay time is the elastic energy, ensuing from the Cu–Au atomic size mismatch.

1. Introduction

Compound-forming alloys such as $Cu_{0.75}Au_{0.25}$ are substitutionally disordered above some temperature T_c and order crystallographically below T_c. The time evolution of order, when such an alloy is quenched from above to below T_c, is a central issue in alloy physics [1–4]. The initial large energy cost associated with nucleating the ordered domain within the metastable disordered region leads to a delay time ('incubation period') in the ordering kinetics. Such a delay has been observed, for example, in Cu_3Au [2–5], CuAu [6], and Mg_3In [7] using time-resolved x-ray scattering experiments and simulations. The present paper focuses on understanding the physics underlying this early time evolution of ordering.

Since nucleation of a particular ordered variant from the disordered medium involves breaking and remaking of chemical bonds in some localized region, this process is often described [8–10] via a short-range Ising-type Hamiltonian representing the chemical (chem) interaction of a single-site (J_1), and between atomic pairs (J_{ij}) or triplets (J_{ijk}) etc, as

$$H_{\text{chem}}(\sigma) = J_0 + J_1 \sum_i S_i(\sigma) + \sum_{j<i} J_{ij} S_i S_j + \sum_{k<j<i} J_{ijk} S_i S_j S_k + \cdots. \quad (1)$$

Here the configuration σ is defined by specifying the occupation of each of the N lattice sites by an A atom or a B atom, via a fictitious spin variable S_i ($i = 1, 2, \ldots, N$), with $S_i = -1$ if site i is occupied by an A atom, and $S_i = +1$ if site i is occupied by a B

atom. Disappointingly, restricting equation (1) to first-nearest-neighbour interactions fails to produce in finite temperature simulations any delay time (nucleation region) [8, 9]. However, introduction of vacancies into a short-ranged Ising Hamiltonian produced a delay time in Monte Carlo simulations [9], promoting the view that nucleation results from vacancies [9]. This scenario, however, does not have a clear physical link to the structure and energetics of metal alloys. In phase-separating systems during nucleation, there is a change in the free energy due to transfer of atoms from a less stable (disorder phase) to a more stable phase (order phase). The difference between the chemical free energies of the disordered and ordered phases supplies the driving force for the transformation. However, if the solvent and the solute atoms have different atomic radii, the ensuing elastic strain energy can reduce this driving force, since the formation of composition fluctuation is associated with the expenditure of elastic free energy [12]. The strain arising from the coexistence of different 'ordered clusters' (Cu_3Au, Cu_2Au_2, $CuAu_3$, etc) with different effective sizes sets up a long-range elastic interaction, absent from the conventional (equation (1)) Ising representation. In the following we will show that such elastic interactions reduce the driving force for ordering, and cause a nucleation step (*i.e., incubation period*) in ordering alloys such as Cu_3Au.

Conventional Ising representations (equation (1)) used in alloy theory [8–11] do not properly capture elastic interactions which are both long ranged and orientation dependent [13, 14]. For example, one often [8–11] truncates the Hamiltonian of equation (1) arbitrarily to include only a couple of pair interactions, often excluding many-body terms. Furthermore, while one could fix the value of nearest-neighbour J_2 pair interaction by fitting to the measured T_c, this fit systematically fails in correctly predicting the compound formation enthalpies, as shown in [14]. Similarly, adjusting the Js to fit the observed short-range-order (SRO) patterns fails to reproduce the measured formation energies [15]. These failures reflect the fact that the determination of T_c and SRO involves fundamentally only the relative energies of iso-compositional phase (e.g., ordered versus disordered, or random versus disordered). In this case the strain in both phases is nearly the same, and thus cancels out in the energy difference. On the other hand, compound formation enthalpies *E(AB)–E(A)–E(B)* as well as nucleation energies involve hetero-compositional configurations (e.g., A-rich versus B-rich A_pB_q clusters), so no cancellation of strain energy terms occurs [14–16].

An alternative approach to study lattice configurational transformations is to perform finite-temperature simulations on a Hamiltonian that is explicitly constructed from a microscopic theory of interatomic cohesion [14, 17]. Here one can write a general Ising-like cluster expansion $E_{CE}(\sigma)$, and determine the number, type, and magnitude of all interaction energies $\{J\}$ by mapping the cluster expansion $E_{CE}(\sigma)$ onto quantum mechanical energies $E_{QM}(\sigma) = \langle\Psi|H|\Psi\rangle/\langle\Psi|\Psi\rangle$ of a few configurations σ. The latter are calculated by, for example, the local density approximation (LDA). It turns out [14] that the mapping $E_{CE} \leftrightarrow E_{QM}(\sigma)$ *forces upon us* the introduction of a strain energy term into the E_{CE}. In general, strain is a consequence of packing onto a lattice atoms of different sizes. We distinguish here two forms of strain [14]. (i) That associated with 'cell-external' degrees of freedom, i.e., the change of lattice vectors. This includes volume changes with composition or changes in the tetragonal c/a ratio when a cubic ($c/a = 1$) fcc-disordered CuAu phase-transforms into the tetragonal CuAu $L1_0$ ordered structure ($c/a \neq 1$). (ii) That associated with 'cell-internal' degrees of freedom, i.e., displacements of atoms within the cell away from their nominal (fcc, bcc, ...) lattice sites. We include cell-internal strain by fitting the cluster expansion (CE) to the calculated total energies in which the atoms are permitted to relax to the nearest local minimum for the structure at hand. Cell-internal relaxation is evident by the fact that in general even in the cubic random alloy the Cu–Cu, Cu–Au and Au–Au distances are unequal. Cell-external strain tends to create long-range interactions [14]. This term represents the atomic displacements associated with

packing atoms of dissimilar sizes onto the lattice. The form

$$H_{\text{strain}}(\sigma) = \sum_{\mathbf{k}} \frac{\Delta E_{\text{cs}}^{\text{eq}}(x, \hat{k})}{4x(1-x)} |S(\mathbf{k}, \sigma)|^2 F(\mathbf{k}) \tag{2}$$

describes such interactions, where $S(\mathbf{k}, \sigma)$ is the Fourier transform of the spin configuration σ, $F(\mathbf{k})$ is an attenuation factor [18], and $\Delta E_{\text{cs}}^{\text{eq}}(x, \hat{k})$ is the coherency-strain term calculated [14] from total energies of the elemental A and B solids deformed elastically in various directions. The total cluster expansion Hamiltonian is

$$E_{\text{CE}}(\sigma) = H_{\text{chem}}(\sigma) + H_{\text{strain}}(\sigma), \tag{3}$$

given by equations (1) and (2). The essential difference between the classical application of Ising models [8–11] and the approaches using the density functional-based cluster expansion [14–19] is that in the former approach the range and magnitudes of the interactions are arbitrarily postulated at the outset, while the latter approach determines the interaction from a microscopic electronic structure theory.

Here we use the first-principles configurational Hamiltonian of equation (3), fitted to the LDA, to study the ordering kinetics of $Cu_{0.75}Au_{0.25}$. For Cu–Au, the interaction energies $\{J\}$ are obtained by fitting equation (3) to 38 LDA calculated total energies $E_{\text{QM}}(\sigma)$ of Cu_pAu_q periodic structures [19]. This automatically yields the non-vanishing pair interactions (about 20) and the many-body terms (about 6) plus an infinite-ranged strain term of equation (2). Without the strain term (2) the fit is qualitatively incorrect for long-period (p, q large) structures [14], and misses the orientation dependence of the formation energies. This Hamiltonian produces, via Monte Carlo (MC) simulations, physically accurate SRO parameters, and order–disorder transition temperatures, as well as the formation enthalpies of various ordered and disordered phases [19].

Applying these different Hamiltonians to ordering kinetics we find several crucial features. (i) $H_{\text{chem}}(\sigma)$ alone produces no delay even if it extends to 20 pair interactions and a few many-body terms. (ii) $H_{\text{chem}}(\sigma) + H_{\text{strain}}(\sigma)$ does produce the observed delay, as noted experimentally [2–4]. We find that $H_{\text{strain}}(\sigma)$ alone is responsible for the delay. (iii) The model predicts that reduction of temperature shortens the delay time, as observed experimentally [3, 4]. We conclude that the existence of an incubation period reflects the existence of long-range interactions. Construction of the cluster expansion from a microscopic (i.e., LDA) theory of cohesion shows that the physical source of long-range interactions in a size-mismatched alloy is elastic, whereas conventional chemical interactions have a short or intermediate range. Thus, elastic energies modify the ordering kinetics.

2. Constructing a cluster expansion and its Monte Carlo simulations

To understand the effects of different physical terms on the ordering kinetics of Cu_3Au we performed separate Monte Carlo simulations with (a) the total Hamiltonian, equation (3), (i.e., chemical + strain), (b) a Hamiltonian with chemical interactions only (equation (2)), and (c) a Hamiltonian where the chemical interactions are reduced to only first-nearest neighbours, as in classic Ising simulations [8, 9]. We fitted our CE to LDA formation energies in cases (a) and (b). The standard deviations of the fits were comparable in both cases. The calculated order–disorder transition temperatures are 518 and 749 K for cases (a) and (b), respectively. The experimental value is 663 K [3]. For case (c) we adjusted the nearest-neighbour J value such that the transition temperature was equal to that obtained in case (a). The calculated ordering spinodal temperatures for cases (a) and (b) are 438, and 638 K, respectively. For both cases (a)

and (b) the spinodal temperature is about 0.85 T_c. The experimental value is 0.96 T_c [20]. In our simulations we work at a temperature (0.77 T_c) *below* this ratio. Note that working below spinodal temperature means that there is no barrier to spinodal (001) ordering.

In all cases the system was quenched from the same disordered configuration to a temperature below the transition temperature. The quenching temperatures in every case were chosen in a such way that the ratio of quenched temperature to transition temperature was the same for all the Hamiltonians. Using Monte Carlo spin-flip dynamics on lattice sites does not mimic the true dynamical evolution of growth, for which, for example, a kinetic algorithm is needed. However, we do not aim at predicting the kinetics path. Rather we aim at predicting the time scaling exponent α of the energy $\Delta E \sim t^{-\alpha}$ [21]. We define unit of time (Monte Carlo step, or mcs) as one spin flip per site for all sites. In this way we shall exploit the dynamical process inherent in the usual Monte Carlo method to construct the time evolution. This allows for a suitable timescale of the kinetics at the expenses of losing the precise proportionality λ between Monte Carlo time and real time. This is not a serious restriction as long as we are interested in the growth exponent α (the slope in a $\ln \Delta E$ versus $\ln t$ plot) which is independent of the time scaling λ (even if it differs at nucleation or growth stages).

To demonstrate the range of interaction of the different Hamiltonians (a)–(c) we calculated the 'pair flip energy', i.e., the energy needed to flip an Au atom at site i and a Cu atom at site j separated by distance R along [110] in the random alloy into a Cu atom at site i and an Au atom at site j. As expected, for the nearest-neighbour Hamiltonian (c) the pair flip energies fall to zero beyond the first nearest-neighbour distance. A pair flip costs more energy, and is longer range in Hamiltonians (a) and (b): for example, for nearest-neighbour distance, pair flip energies for cases (a) and (b) are 23% and 25% higher than for case (c), respectively. For a third-neighbour separation the flip energies are 14.5 and -0.8 meV/atom for (a) and (b), while for fifth-neighbour separation they are 8.3 and 2.6 meV/atom. Thus, the driving force for nucleation (the difference between the energy of the quenched-in, homogeneous disordered phase, and the configuration having ordered domains) is reduced in case (a) relative to the other cases.

Figure 1 shows the time evolution of $L1_2$ ordered domains in Cu_3Au system for the early and late stages of growth. The $L1_2$ Cu_3Au structure consists of a coherent repetition of a basic tetrahedron whose four vertices are occupied by Au, Cu, Cu, and Cu; so four different orientational variants (bottom of figure 1) can nucleate. These form individual domains (each shown in figure 1 by a different colour), separated by domain walls ('anti-phase boundaries'). Additionally, off-stoichiometric domains (i.e., clusters, $Cu_{4-p}Au_p$ with $p \neq 1$) can nucleate. Such off-stoichiometric domains are shown in figure 1 by black regions. We see in figure 1 two types of domain wall [22]. The first is the boundary between domains shown in figure 1 with different colours. This type of domain wall conserves the nearest-neighbour configuration (i.e., the concentration Cu_3Au is maintained even locally). The second type of domain wall is shown as black regions and is characterized by the local composition that is off-stoichiometric ($X_{Au} \neq 0.25$) and is non-conserving. Such 'composition fluctuations' cost strain energy; including H_{strain} in the Hamiltonian thus raises the energy of this phase. At early times (top row in figure 1) the percentage of the black region for the Hamiltonian (a) (21%) is higher than that in Hamiltonians (b) (17%) and (c) (8%). That is, the presence of strain energy slows down the growth of ordered $L1_2$ domains in the Cu_3Au system. At long times (bottom row in figure 1) all three Hamiltonians (a)–(c) show large conserving domains, with small non-conserving domains. However, the three Hamiltonians differ at short times: the average domain size is much smaller when strain energy is included in Hamiltonian (a) relative to the cases (b) and (c), where only chemical interactions are included. Therefore, the system in which strain energy is included spends more time in the nucleation process (incubation period) than strain-free systems.

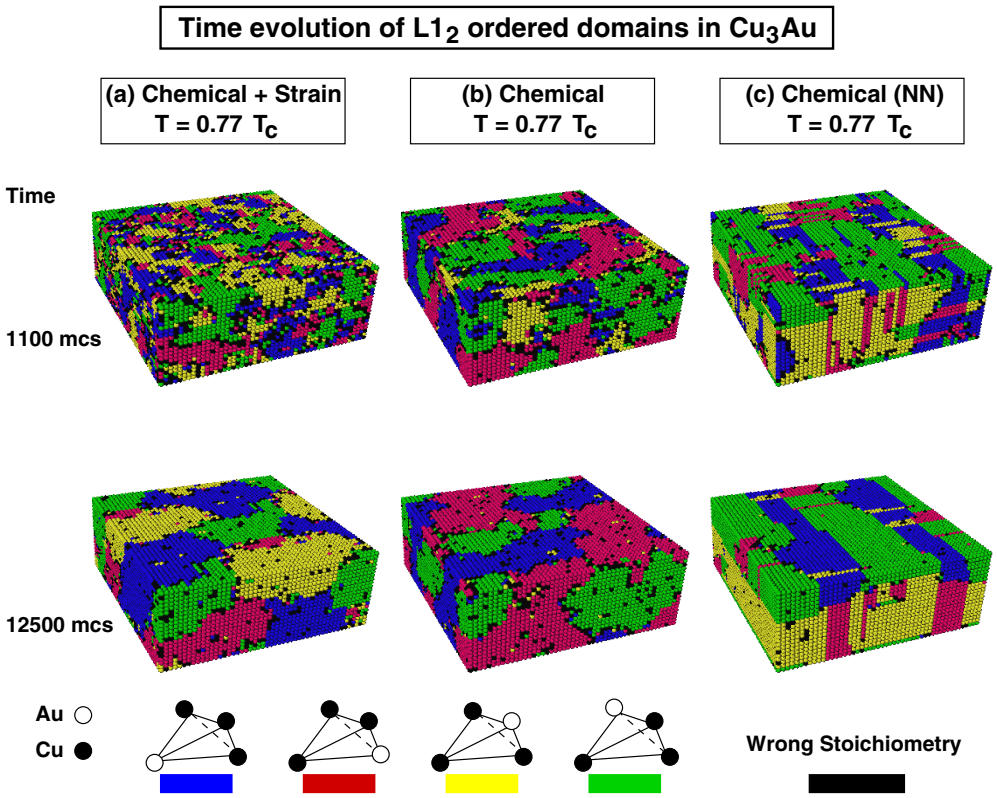

Figure 1. Time evolution of $L1_2$ ordered domains in Cu_3Au alloy for different Hamiltonians at early and late stages of growth at $T = 0.77T_c$ below the spinodal temperature ($T_{spinodal} = 0.85T_c$). (a) $H_{chem} + H_{strain}$, equation (3); (b) H_{chem}, equation (1); (c) $H_{chem}(NN)$ including only first-nearest-neighbour pairs. The bottom part shows the four variants of Cu_3Au. Each tetrahedron is depicted as a different colour in this figure. Black domains denote areas whose composition differs from Cu_3Au.

To extract exponents for nucleation versus growth stages, we calculate the excess energy per site defined as[3]

$$\Delta E(t) = E(t) - E(\infty). \tag{4}$$

Figure 2 depicts a logarithmic plot of $\Delta E(t)$ versus Monte Carlo time (mcs) t at constant temperature ($T = 0.77T_c$). This temperature is below the predicted spinodal temperature ($T_{spinodal} = 0.85T_c$). While the time evolution of the growth stage is known to be a universal power law [23] $R(t) \sim t^{1/2}$ (or $\Delta E(t) \sim t^{1/2}$), where $R(t)$ is the average domain size, the time evolution during the crucial nucleation stage is far less understood [2–4, 6–9]. Figure 2 demonstrates several important results.

[3] The power-law dependence of $R(t)$ and $\Delta E(t)$ on time implies that $R(t)$ and $\Delta E(t)$ are finite for any finite time, and, therefore, that the infinite system does not reach true equilibrium in any finite time. It grows continuously. However, in Monte Carlo simulations and experiments we are dealing with finite systems, and therefore after a finite time the system will be saturated and domain growth stops. In our simulation with 125 000 atoms this saturation is happening around 15 000 *mcs*, and we measured the excess energy of the system at each time with respect to the energy at this time.

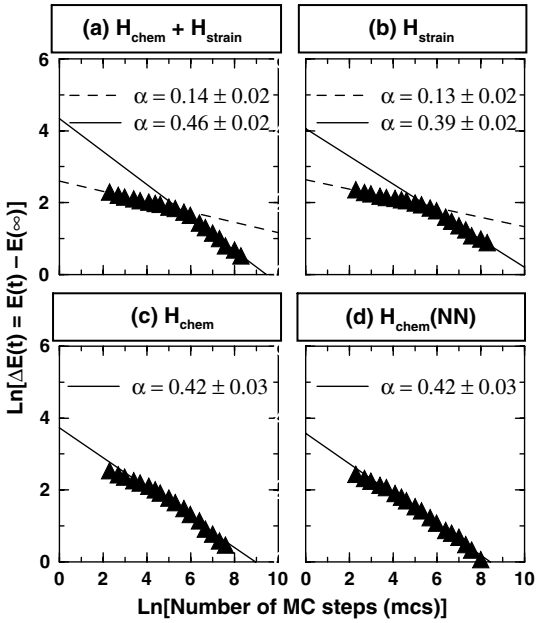

Figure 2. Time evolution of Monte Carlo energy at constant temperature ($T = 0.77T_c$) below the spinodal ($T_{spinodal} = 0.85T_c$) for different Hamiltonians. Only a Hamiltonian with strain energy produces a delay time.

(i) At the growth stage the simulations of all of our Hamiltonians (a)–(c) show $\Delta E(t) \sim t^{-\alpha}$ with $\alpha = 0.4$–0.5. This scaling is consistent with experimental results [3, 4] and standard simulations [8–10].

(ii) A delay time is observed for the Hamiltonian (a) that includes strain energy (figures 2(a), (b)). In this incubation period the domains grow at a smaller rate, i.e., with a power of $\alpha = 0.14 \pm 0.02$. The value of the exponent in this region is in agreement with the generalized nucleation theory of Binder and co-workers [24] based on a numerical solution of Fisher's cluster model. It is also consistent with the numerical simulation of the nonlinear Gibbs–Thomson equation developed by Kampmann and Wagner [25] in which nucleation, growth, and coarsening are treated as a single growth process with different exponents within the framework of classical nucleation and growth theories.

(iii) The use of strain energy in the Hamiltonian (figure 2(b)) is sufficient to produce a delay time giving $\alpha = 0.13 \pm 0.02$ at short times. This provides direct evidence that relates the strain energy to the incubation period.

(iv) The chemical energy part of Hamiltonian (a) varies like a straight line with respect to time. Although a hypothetical infinite-range chemical Hamiltonian could produce a delay time, our theory shows that elastic interactions are the physical source of long-rangedness, whereas the chemical terms have an intermediate range. Thus, realistic chemical Hamiltonians (figures 2(c), (d)) do not produce any delay time, yielding instead large α values[4].

[4] The small deviation from linearity seen in figure 2(c) is directly related to the finite size effects [9]. Fitting the curve in figure 2(c) by two lines gives the exponents for early and late times of 0.36 and 0.50, respectively. These values are still much larger than 0.14 and indicate a growth rather than a nucleation region for pure chemical Hamiltonians.

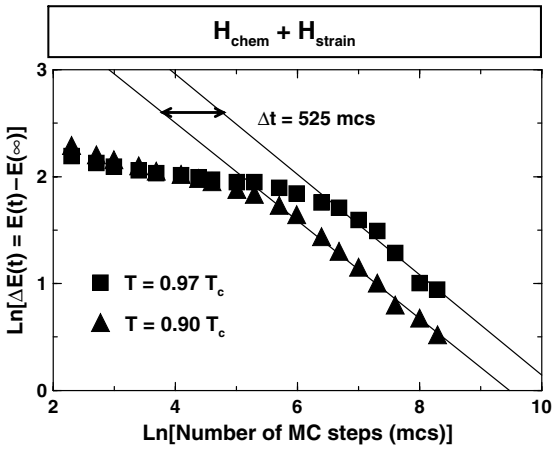

Figure 3. Time evolution of Monte Carlo energy at two different temperatures above the spinodal ($T_{\text{spinodal}} = 0.85T_{\text{c}}$) for the full Hamiltonian ($H_{\text{chem}} + H_{\text{strain}}$). Note how the delay time is reduced by lowering the temperature.

It was found experimentally that as the quench temperature decreases (above the spinodal temperature) the timescale for nucleation becomes shorter in the Cu_3Au system [3, 4]. To examine whether Monte Carlo simulations can give similar results, we performed simulations with the same chemical + strain Hamiltonian (a) at different temperatures above the spinodal temperature $T_{\text{spinodal}} = 0.85T_{\text{c}}$. In figure 3 we show two results, at $T = 0.90T_{\text{c}}$ and $0.97T_{\text{c}}$. As expected from our model, we see that the delay time decreases (here, by 66%) by reducing the quench temperature. This shows that the results for our Hamiltonian qualitatively agree with experiment. Further simulations at different temperatures below the spinodal temperature ($0.77T_{\text{c}}$, and $0.57T_{\text{c}}$) showed the presence of the nucleation region, which in reality can be so small that it is not detected experimentally. Another important factor which can affect the nucleation process is the presence of the vacancies in the alloy. Figure 2(b) shows that the nucleation process is completely controlled by the strain part of the Hamiltonian (a) and that the presence of the vacancies can reduce the strain energy and shorten the incubation period.

We have emphasized in this work that the inclusion of both the cell-internal and the cell-external terms in the Hamiltonian leads, at temperatures below the spinodal, to a delay time for nucleation (distinct from the delay associated with spinodal barriers, observable at temperatures above the spinodal). Chakraborty and Xi [5] have used Monte Carlo simulations of the short-time and long-time evolution of ordering in Cu_3Au, retaining only the cell-external (c/a variation) term. Their work uses a different description of the energetics of the alloy. Specifically, they use the empirical effective medium energy expression of Nørskov *et al* [26], whereas we use first-principles density functional total energies of many different configurations [14]. They present results *above* the spinodal temperatures, where their calculated structure factor as a function of time for $T = 0.972T_{\text{c}}$, is in good agreement with the experiment of [3] up to 22 s. This behaviour is controlled by the existence of activation barriers due to the fact that the spinodal temperature has not yet been reached. However, the important dynamics related to nucleation occurs at temperatures *below* the spinodal. They provide results just for one such temperature, specifically at $T = 0.953T_{\text{c}}$, which is only 3 K below their spinodal temperature. Unfortunately, at this temperature their results disagree with the experiment [3]. The domains appear to order much more quickly than in experiment (according to experiment [3], the structure factors at that temperature range are almost the

same as for $T = 0.973T_c$ up to 40 s, yet the simulation of Chakraborty and Xi starts to differ from $T = 0.972T_c$ already after 10 s). With this fast reduction of delay time evident in their simulations, one would expect that for temperatures well below (more than just 3 K) the spinodal temperature (namely our figures 1 and 2), they will not be able to represent any substantial nucleation delay time. It is not obvious if this main discrepancy between their work and ours results from differences in the description of cell-external strain (effective medium in [5] versus density functional fit cluster expansion in the present work) or from the fact that cell-internal strain is not included in the work of [5].

3. Conclusion

Previous Monte Carlo simulations of the nearest-neighbour Ising model showed [8, 9] that after quenching there is immediate growth with an average domain size growing as $R(t) \sim t^{1/2}$ ($\Delta E \sim t^{-1/2}$). However, time-resolved x-ray scattering experiments [2–4] showed that the crossover to the simple $t^{1/2}$ growth behaviour occurs only after an incubation period. We have shown that a Monte Carlo simulation of a realistic (first-principles derived) Hamiltonian that, by necessity, includes strain, produces the delay (incubation period) in the early times. We have demonstrated that the strain energy is directly responsible for this delay time.

Acknowledgments

This work is supported by the Advanced Research Program of the State of Texas and US Department of Energy, SC-BES-OER through NREL contract No. DE-AC36-98-GO10337.

References

[1] Cahn R W 1987 *Mater. Res. Soc. Symp. Proc.* **57** 385
Noda Y, Nishihara S and Yamada Y 1984 *J. Phys. Soc. Japan* **45** 4241
[2] Nagler S E, Shannon R F Jr, Harkless C R, Singh M A and Nicklow R M 1988 *Phys. Rev. Lett.* **61** 718
[3] Ludwig K F Jr, Stephenson G B, Jorda-Sweet J L, Mainville J, Yang Y S and Sutton M 1988 *Phys. Rev. Lett.* **61** 1859
[4] Shannon R F Jr, Nagler S E and Harkless C R 1992 *Phys. Rev.* B **46** 40
[5] Chakraborty B and Xi Z 1996 *Phys. Rev.* B **53** 5063
[6] Malis O and Ludwig K F Jr 1999 *Phys. Rev.* B **60** 14675
[7] Konishi H and Noda Y 1988 *Dynamics of Ordering Processes* ed S Komura (New York: Plenum)
[8] Phani M K, Lebowitz J L, Kalos M H and Penrose O 1980 *Phys. Rev. Lett.* **45** 366
[9] Frontera C, Vives E, Castán T and Planes A 1997 *Phys. Rev.* B **55** 212
[10] Styer D F, Phani M K and Lebowitz J L 1986 *Phys. Rev.* B **34** 3361
Phani M K, Lebowitz J L and Kalos M H 1980 *Phys. Rev.* B **21** 4027
Düuweg B and Binder K 1987 *Phys. Rev.* B **36** 6935
Finel A, Mazauric V and Ducastelle F 1990 *Phys. Rev. Lett.* **65** 1016
[11] Berley D M 1972 *Phase Transition and Critical Phenomena* ed C Domb and M S Green (London: Academic) p 329
[12] Cahn J W 1962 *Acta Metall.* **10** 907
[13] Cook H E and de Fontaine D 1971 *Acta Metall.* **19** 607
Khachturyan A G 1983 *Theory of Phase Transformations in Alloys* (New York: Wiley)
[14] Zunger A 1994 *Statics and Dynamics of Alloy Phase Transformation* ed P E A Turchi and A Gonis (New York: Plenum)
Laks D B, Froyen S, Ferreira L G and Zunger A 1992 *Phys. Rev.* B **46** 12578
[15] Wolverton C and Zunger A 1997 *Solid State Commun.* **101** 519
[16] Zunger A, Wei S-H, Mbaye A A and Ferreira L G 1988 *Acta Metall.* **36** 2239
[17] Connolly J W D and Williams A R 1983 *Phys. Rev.* B **27** 5169
[18] Wolverton C, Ozoliņš V and Zunger A 2000 *J. Phys.: Condens. Matter* **12** 2749

[19] Ozoliņš V, Wolverton C and Zunger A 1998 *Phys. Rev.* B **57** 6427
Wolverton C, Ozoliņš V and Zunger A 1998 *Phys. Rev.* B **57** 4332
[20] Gaulin B D, Hallman E D and Svensson E C 1990 *Phys. Rev. Lett.* **64** 289
[21] Sadiq A and Binder K 1983 *Phys. Rev. Lett.* **51** 674
[22] Kikuchi R and Cahn J W 1979 *Acta Metall.* **27** 1337
Leroux C, Loiseau A, Cadeville M C, Broddin D and Van Tendeloo G 1990 *J. Phys.: Condens. Matter* **2** 3479
[23] Cahn J W and Hilliard J E 1958 *J. Chem. Phys.* **28** 258
Allen S M and Cahn J W 1979 *Acta Metall.* **27** 1085
[24] Binder K, Billotet C and Mirold C 1978 *Z. Phys.* B **30** 183
[25] Kampmann R and Wagner R 1984 *Decomposition of Alloys: The Early Stages* ed P Hassen, V Gerold, R Wagner and M F Ashby (Oxford: Pergamon)
[26] Nørskov J K, Jacobsen K W and Puska M J 1987 *Phys. Rev.* B **35** 7423